

ACTIVE SITES FOR ADSORPTION OF  $\beta$ -CAROTENE

by

TAN SIAM HWA

Thesis submitted in fulfilment of the requirement for  
the degree

Master of Science

March 1982

CONTENTS

	<u>Page</u>
List of Tables	vii
List of Figures	x
Abstract ( Bahasa Malaysia )	xiv
Abstract ( English )	xvii
<u>Chapter 1</u> Introduction	
1. Objective	1
2. Refining of Crude Palm Oil	2
(a) Bleaching of Palm oil	4
(b) Bleaching Earths	6
3. Zeolites	14
(a) Crystal Structure of X and Y Zeolites	16
(b) Properties of X and Y Zeolites	19
(c) Transition Metal Ions in Zeolites	26
4. Adsorption of Solids from Solution	27
(a) Experimental Data of Adsorption	30
<u>Chapter 2</u> Experimental	
1. Materials	33
2. Preparation of Cation Exchanged Zeolites	34

	<u>Page</u>
3. Preparation of Cation Exchanged Clays	37
(a) Preparation of Na Exchanged Clays	37
(b) Preparation of H, Fe, Mg and Ca Exchanged Clays	38
4. Sample Treatment	
(a) For Adsorption	43
(b) For Bleaching Test	43
5. Adsorption Study	
(a) Rate of Adsorption of $\beta$ -carotene	43
(b) Adsorption Isotherm	44
(c) Calibration of $\beta$ -carotene	45
6. Bleaching of Crude Palm Oil with Cation Exchanged Clays	
(a) Bleaching Test	46
7. X-Ray Powder Diffraction of Zeolites and Clays	47
8. Surface Area Measurement by BET Method	49
9. Surface Acidity Measurement by Nonaqueous Titration	50
10. Preliminary Investigation of reaction products from $\beta$ -carotene and CuNaY zeolite	52
<u>Chapter 3</u> Adsorption of $\beta$ -carotene by Cation Exchanged Zeolites	
1. Introduction	54
2. Results and Discussion	
(a) Alkali     and Alkaline Earth Zeolites	55

(b) HNaY and MNaX Zeolites	56
(c) Fe(III)NaY and Fe(III)NaX Zeolites	64
(d) Cu(II)NaY and Cu(II)NaX Zeolites	73
(e) Preliminary Analysis of the Products formed from the Reaction of $\beta$ -carotene with Cu(II)NaY Zeolites	85
3. General Discussion	92
4. Conclusion	97

Chapter 4      Adsorption of  $\beta$ -carotene by Cation Exchanged  
Bleaching Earths

1. Introduction	100
2. Results and Discussion	101
3. Conclusion	128

Chapter 5      Bleaching of Crude Palm Oil with Cation  
Exchanged Bleaching Earths

1. Introduction	130
2. Results and Discussion	
(a) Colour	132
(b) Free Fatty Acids Content	140
(c) Peroxide Value	142
(d) Anisidine Value and Tortox Value	153
(e) Phosphorous Value	154
(f) Iron Content	154
3. Conclusion	155

## Appendix I

1. Determination of Free Fatty Acid Content in Palm Oil	157
2. Determination of Peroxide Value in Palm Oil	158
3. Determination of Anisidine Value in Palm Oil	158
4. Determination of Phosphorus Content in Palm Oil	160
5. Determination of Iron Content in Palm Oil	162

## Appendix II Numerical Data of Adsorption Study

1. Cation Exchanged Zeolites	164
2. Cation Exchanged Clays	176

References	184
------------	-----

List of Tables

	<u>Page</u>
Table 2.1: Preparation of various Cation Exchanged Zeolites.	35
Table 2.2: Concentrations of various Cations Exchanged by Sodium ion in the three types of Clays.	40
Table 2.3: Preparation of various Cation Exchanged Clays and their Extent of Exchange for Sodium ions.	41
Table 2.4: Filtrol-Clay with various Extent of Exchange of Hydrogen and Iron for Sodium ions.	42
Table 3.1: Acidity of Cation Exchanged Zeolites using Triphenylmethanol Indicator ( $pK_{R^+} = -6.63$ ) ( Acid Strength: 50 wt % $H_2SO_4$ ).	61
Table 3.2: Crystal Structure Retention of Cation Exchanged Zeolites Determined by X-ray Powder Diffraction.	69
Table 3.3: Surface Area of Cation Exchanged Zeolites Determined by BET Method.	70
Table 3.4: Mass Spectra Data of Unknown Adsorbed Compounds.	91
Table 4.1: Surface Area of Cation Exchanged Filtrol Determined by BET Method.	111
Table 4.2: Acidity of Cation Exchanged Filtrol using Triphenylmethanol Indicator ( $pK_{R^+} = -6.63$ ) ( Acid Strength: 50 wt % $H_2SO_4$ ).	122
Table 5.1: Physical Characteristics of Crude Palm Oil.	133
Table 5.2: Various Cation Exchanged Clays used for Bleaching Crude Palm Oil.	134

	<u>Page</u>
Table 5.3: Bleaching of CPO with Original Filtrol.	143
Table 5.4: Bleaching of CPO with Na-Filtrol.	144
Table 5.5: Bleaching of CPO with Original Galleon.	145
Table 5.6: Bleaching of CPO with Na-Galleon.	146
Table 5.7: Bleaching of CPO with H-Filtrol.	147
Table 5.8: Bleaching of CPO with Fe-Filtrol.	148
Table 5.9: Bleaching of CPO with H-Galleon.	149
Table 5.10: Bleaching of CPO with Fe-Galleon.	150
Table 5.11: Bleaching of CPO with Mg-Filtrol.	151
Table 5.12: Bleaching of CPO with Ca-Filtrol.	152

List of Figures

	<u>Page</u>
Figure 1.1:	8
(a) A single octahedral and (b) The sheet structure of the octahedral units.	
Figure 1.2:	8
(a) A single tetrahedron and (b) The sheet structure of silica tetrahedra, arranged in a hexagonal network.	
Figure 1.3:	9
Arrangement of Octahedral and Tetrahedral Sheets to form the Montmorillonite Structure.	
Figure 1.4:	13
Idealised Structure of Acid-Activated Montmorillonite.	
Figure 1.5:	18
(a) Sodalite Cage. (b) Supercage of Faujasite Type. (c) Arrangement of Sodalite Cages to give Faujasite Structure.	
Figure 1.6:	28
Typical Shape of Isotherm for Adsorption of a Solid from Solution.	
Figure 1.7:	31
Classification of Isotherm by Giles.	
Figure 3.1:	58
Rate of Adsorption of $\beta$ -carotene by 88.0% HNaY at various temperatures. (a) 10°C (b) 20°C (c) 30°C and (d) 40°C.	
Figure 3.2:	59
Apparent Adsorption Isotherms of $\beta$ -carotene by HNaY with various Extent Exchange at 25°C. (a) 30.0% (b) 43.0% (c) 66.0% and (d) 88.0%.	
Figure 3.3:	62
Apparent Adsorption Isotherms of $\beta$ -carotene by 60.0% HNaX at 25°C. (a) Calcined at 450°C and (b) Calcined at 550°C.	
Figure 3.4:	65
Activity of Cation Exchanged Zeolites vs Extent of Exchange at 25°C. (a) HNaY and (b) Fe(III)NaY.	



	<u>Page</u>
Figure 3.5: Rate of Adsorption of $\beta$ -carotene by 32.5% Fe(III)NaY at 25°C.	66
Figure 3.6: Apparent Adsorption Isotherms of $\beta$ -carotene at 25°C. (a) 8.8% (b) 13.8% (c) 20.0% and (d) 32.5%.	68
Figure 3.7: Apparent Adsorption Isotherms for Fe(III)NaX with various Extent EXchange at 25°C. (a) 23.8% (b) 37.5% and (c) 60.0%.	72
Figure 3.8: Rate of Adsorption of $\beta$ -carotene by 71.0% Cu(II)NaY at (a) 25°C and (b) 40°C.	74
Figure 3.9: Rate of Adsorption of $\beta$ -carotene by 52.4% Cu(II)NaY at various temperatures. (a) 10°C (b) 20°C (c) 30°C and (d) 40°C.	76
Figure 3.10: Arrhenius Plot for Adsorption of $\beta$ -carotene by 52.4% Cu(II)NaY.	77
Figure 3.11: Apparent Adsorption Isotherms of $\beta$ -carotene by Cu(II)NaX with various Extent of Exchange at 25°C. (a) 18.0% (b) 35.0% and (c) 51.3%.	79
Figure 3.12: Apparent Adsorption Isotherms of $\beta$ -carotene by Cu(II)NaY with various Extent of Exchange at 25°C. (a) 13.6% (b) 22.8% (c) 40.6% (d) 52.4% and (e) 71.0% .	80
Figure 3.13: Activity of Cation Exchanged Zeolites vs Extent of Exchange at 25°C. (a) HNaY (b) Fe(III)NaY (c) Cu(II)NaY and (d) Cu(II)NaX.	81
Figure 3.14: Apparent Adsorption Isotherm of $\beta$ -carotene by 91.0% Cu(II)NaY at 25°C.	84
Figure 3.15: UV Spectrum of compound I or II in pet. ether.	88
Figure 3.16: IR Spectrum of Chloroform Extract.	90

	<u>Page</u>
Figure 4.1:	X-ray Powder Diffractogram of Original Filtrol Clay. Mont, Montmorillonite; M, Mica; Q, Quartz; K, Kaolinite. 102
Figure 4.2:	X-ray Powder Diffractogram of Original Fulmont Clay. Mont, Montmorillonite; M, Mica; Q, Quartz; K, Kaolinite. 103
Figure 4.3:	X-ray Powder Diffractogram of Original Galleon Clay. Mont, Montmorillonite; M, Mica; Q, Quartz; Cr, Cristobalite. 104
Figure 4.4:	X-ray Powder Diffractogram of H-Filtrol Clay ( $25.7 \times 10^{-2}$ meq $g^{-1}$ ) heated at $450^{\circ}C$ for 4 hours. Mont, Montmorillonite; M, Mica; Q, Quartz. 105
Figure 4.5:	X-ray Powder Diffractogram of Fe-Filtrol Clay ( $25.5 \times 10^{-2}$ meq $g^{-1}$ ) heated at $450^{\circ}C$ for 4 hours. Mont, Montmorillonite; M, Mica; Q, Quartz. 106
Figure 4.6:	X-ray Powder Diffractogram of Mg-Filtrol Clay ( $20.9 \times 10^{-2}$ meq $g^{-1}$ ) heated at $450^{\circ}C$ for 4 hours. Mont, Montmorillonite; M, Mica; Q, Quartz. 107
Figure 4.7:	X-ray Powder Diffractogram of Ca-Filtrol Clay ( $21.5 \times 10^{-2}$ meq $g^{-1}$ ) heated at $450^{\circ}C$ for 4 hours. Mont, Montmorillonite; M, Mica; Q, Quartz. 108
Figure 4.8:	X-ray Powder Diffractogram of Filtrol Clay treated with 0.1M NaOH and heated at $450^{\circ}C$ for 4 hours. Mont, Montmorillonite; M, Mica; Q, Quartz. 109
Figure 4.9:	Apparent Adsorption Isotherms of $\beta$ -carotene Bleaching Earths at $25^{\circ}C$ . (a) Original Galleon (b) Original Filtrol and (c) Original Fulmont. 113
Figure 4.10:	Apparent Adsorption Isotherms of $\beta$ -carotene by Treated Filtrol samples. (a) Water washed (b) once exchanged with $Na^{+}$ (c) twice exchanged with $Na^{+}$ (d) thrice exchanged with $Na^{+}$ and (e) treated with 0.1M NaOH. 115

	<u>Page</u>
Figure 4.11: Apparent Adsorption Isotherms of $\beta$ -carotene by Cation Exchanged Filtrol Clays. (a) Cu-Filtrol ( $14.4 \times 10^{-2}$ meq $g^{-1}$ ) (b) Fe-Filtrol ( $13.6 \times 10^{-2}$ meq $g^{-1}$ ) and (c) H-Filtrol ( $16.0 \times 10^{-2}$ meq $g^{-1}$ ).	117
Figure 4.12: Activity of Cation Exchanged Filtrol vs Extent of Exchange. (a) H-Filtrol and (b) Fe-Filtrol.	119
Figure 4.13: Apparent Adsorption Isotherms of $\beta$ -carotene by (a) Ca-Filtrol ( $26.1 \times 10^{-2}$ meq $g^{-1}$ ) and (b) Mg-Filtrol ( $25.9 \times 10^{-2}$ meq $g^{-1}$ ).	120
Figure 4.14: Apparent Adsorption Isotherms of $\beta$ -carotene by Cation Exchanged Fulmont Clays. (a) Na-Fulmont (b) Ca-Fulmont ( $22.8 \times 10^{-2}$ meq $g^{-1}$ ) (c) H-Fulmont ( $27.5 \times 10^{-2}$ meq $g^{-1}$ ) (d) Fe-Fulmont ( $24.3 \times 10^{-2}$ meq $g^{-1}$ ) and (e) Mg-Fulmont ( $25.0 \times 10^{-2}$ meq $g^{-1}$ ).	124
Figure 4.15: Apparent Adsorption Isotherms of $\beta$ -carotene by Cation Exchanged Galleon Clays. (a) Na-Galleon (b) Ca-Galleon ( $20.9 \times 10^{-2}$ meq $g^{-1}$ ) (c) H-Galleon ( $25.4 \times 10^{-2}$ meq $g^{-1}$ ) (d) Fe-Galleon ( $23.0 \times 10^{-2}$ meq $g^{-1}$ ) and (e) Mg-Galleon ( $21.7 \times 10^{-2}$ meq $g^{-1}$ ).	125
Figure 4.16: Amount of $\beta$ -carotene adsorbed by Original Filtrol as a function of Time at (a) $20^{\circ}C$ and (b) $30^{\circ}C$ .	127
Figure 5.1: Colour of Bleached Oil vs Dosage of Bleaching Earth. (a) Original Filtrol and (b) Na-Filtrol.	136
Figure 5.2: Colour of Bleached Oil vs Dosage of Bleaching Earth. (a) Original Galleon and (b) Na-Galleon.	137
Figure 5.3: Colour of Bleached Oil vs Dosage of Bleaching Earth. (a) H-Filtrol and (b) Fe-Filtrol.	138
Figure 5.4: Colour of Bleached Oil vs Dosage of Bleaching Earth. (a) Fe-Galleon and (b) H-Galleon.	139
Figure 5.5: Colour of Bleached Oil vs Dosage of Bleaching Earth. (a) Mg-Filtrol and (b) Ca-Filtrol.	141

Abstrak

Tabii tapak aktif dalam aluminosilikat untuk penjerapan  $\beta$ -karotena telah diperiksakan. Zeolit bertukaran kation mempunyai berbagai darjat pertukaran  $\text{NH}_4^+$ ,  $\text{Mg}^{2+}$ ,  $\text{Ca}^{2+}$ ,  $\text{Fe}^{3+}$  dan  $\text{Cu}^{2+}$  telah disediakan. Kehabluran sampel-sampel itu selepas diaktifkan pada  $450^\circ\text{C}$  telah diperiksakan oleh difrakse sinar X dan luas permukaan ditentukan dengan penjerapan  $\text{N}_2$  (BET). Keasidan permukaan sampel ini juga ditentukan oleh pentitratan tak-berair dengan menggunakan penunjuk trifenilmetanol.

Isoterm penjerapan kentara  $\beta$ -karotena dalam aseton oleh zeolit bertukaran kation yang diaktifkan telah didapatkan pada suhu bilik. Aktiviti-aktiviti penjerapan bertambah dengan penambahan dalam takat pertukaran ion  $\text{Na}^+$  untuk ion-ion  $\text{NH}_4^+$ ,  $\text{Fe}^{3+}$  dan  $\text{Cu}^{2+}$ . Tetapi tidak ada aktiviti diperhatikan untuk zeolit bertukaran  $\text{Na}^+$ ,  $\text{Mg}^{2+}$  dan  $\text{Ca}^{2+}$ . Turutan aktiviti telah didapati sebagai :  $\text{Cu}^{2+} > \text{Fe}^{3+} > \text{H}^+ \gg \text{Mg}^{2+} \sim \text{Ca}^{2+} \sim \text{Na}^+$ . Penyingkiran  $\beta$ -karotena oleh zeolit bertukaran kation melibatkan suatu proses penjerapan kimia yang cepat pada awalnya berikutan dengan suatu tindakbalas tertib zero. Dalam  $\text{Cu(II)NaY}$ , tenaga pengaktifan kentara untuk tindakbalas tertib zero itu ialah  $9.94 \text{ kcal mol}^{-1}$ .

Keasidan Bronsted dan ion-ion logam peralihan telah dicandangkan sebagai pusat aktif. Dalam  $\text{HNaY}$  dan  $\text{HNaX}$ , aktiviti itu berasal

daripada tapak asid Bronsted.  $MgNaX$  dan  $CaNaX$  tidaklah aktif oleh sebab tapak Bronstednya bertempat dikedudukan yang tidak dapat didatangi. Zeolit ion logam peralihan adalah sangat aktif berbanding dengan zeolit hidrogen. Ion-ion logam peralihan telah diusulkan sebagai pusat aktif utama dalam zeolit-zeolit ini. Pemerhatian masa aruhan kinetik dan pengasingan hasil pengoksidaan memberikan bukti tambahan bahawa ion logam peralihan seperti  $Cu^{2+}$  adalah terlibat dalam penyingkiran  $\beta$ -karotena oleh zeolit itu.

Aktiviti-aktiviti zeolit ion logam peralihan tidak bertambah secara linear dengan penambahan pertukaran. Keterangan yang telah dikemukakan adalah kedudukan kation itu tidak dapat didatangi pada pertukaran rendah. Zeolit jenis X telah didapati lebih aktif daripada zeolit jenis Y. Kelakuan ini telah dibincangkan dalam sebutan keadaan tapak kation yang tidak dipenuhi dan tapak asid Lewis.

Kajian ini telah dilanjutkan untuk meliputi beberapa tanah peluntur bertukaran kation. Kebolehan beberapa kation dalam menyampaikan aktiviti untuk penjerapan  $\beta$ -karotena adalah ditunjukkan seperti berikut :  $H^+ \sim Fe^{3+} \sim Mg^{2+} > Ca^{2+} > Na^+$ . Aktiviti-aktiviti ini dianggap berasal daripada pusat-pusat asid dan ion-ion logam peralihan seperti  $Fe^{3+}$  dan  $Cu^{2+}$  di atas permukaan tanah. Aktiviti-aktiviti ini didapati bertambah secara linear dengan penambahan dalam pertukaran.

Tanah peluntur bertukaran kation juga digunakan untuk meluntur minyak kelapa sawit dibawah keadaan piawai. Keputusan-keputusan menunjukkan bahawa tanah peluntur mempunyai dua fungsi yang penting. Pertama, penyingkiran sebatian-sebatian berwarna dalam minyak kelapa sawit dan kedua, penyingkiran atau "pembersihan" bendasing, umpamanya, peroksida, fosfatida dan logam-logam berat. Telah juga didapati bahawa aktiviti tanah peluntur bertukaran kation terhadap pengurangan warna dan "pembersihan" bendasing itu mengikuti aliran yang sama, iaitu, ion-ion  $H^+$ ,  $Fe^{3+}$  dan  $Mg^{2+}$  menyampaikan aktiviti yang tinggi tetapi ion-ion  $Ca^{2+}$  dan  $Na^+$  menyampaikan aktiviti yang rendah pada tanah peluntur.

ABSTRACT

The nature of active sites in aluminosilicates for the adsorption of  $\beta$ -carotene was investigated. Cation exchanged zeolites with varying extent of exchange of  $\text{NH}_4^+$ ,  $\text{Mg}^{2+}$ ,  $\text{Ca}^{2+}$ ,  $\text{Fe}^{3+}$ , and  $\text{Cu}^{2+}$  were prepared. The crystallinity of these samples activated at  $450^\circ\text{C}$  were checked by x-ray diffraction and the surface areas were determined by  $\text{N}_2$  adsorption (BET). The surface acidities of the samples were also determined by nonaqueous titration using triphenylmethanol indicator.

Apparent adsorption isotherms of  $\beta$ -carotene in acetone by activated cation exchanged zeolites were obtained at ambient temperature. The adsorption activities increased with the increase in the extent of exchange of  $\text{Na}^+$  ion for  $\text{NH}_4^+$ ,  $\text{Fe}^{3+}$  and  $\text{Cu}^{2+}$  ions. However, no activity was observed for  $\text{Na}^+$ ,  $\text{Mg}^{2+}$  and  $\text{Ca}^{2+}$  exchanged zeolites. The order of activities was found to be:  $\text{Cu}^{2+} > \text{Fe}^{3+} > \text{H}^+ \gg \text{Mg}^{2+} \sim \text{Ca}^{2+} \sim \text{Na}^+$ . The removal of  $\beta$ -carotene by the cation exchanged zeolites involved an initial rapid chemisorption process followed by a zero order reaction. In  $\text{Cu(II)NaY}$ , the apparent activation energy for the zero order reaction was  $9.94 \text{ kcal mol}^{-1}$ .

Bronsted acidity and transition metal ions were proposed to be the active centres. In  $\text{HNaY}$  and  $\text{HNaX}$ , the activities are due to the Bronsted acid sites.  $\text{MgNaX}$  and  $\text{CaNaX}$  are not active because the Bronsted acid are located in inaccessible positions. Transition

metal ion zeolites were very active compared to the hydrogen forms. The transition metal ions were suggested to be the principal active centres in these zeolites. The observation of the kinetic induction period and the isolation of oxidation products for Cu(II)NaY provided additional evidence that the transition metal ions such as  $\text{Cu}^{2+}$  are involved in the removal of  $\beta$ -carotene by the zeolite.

The activities of the transition metals ion zeolites did not increase linearly with the increase in the extent of exchange. The explanation advanced was the location of the cation at inaccessible sites at low exchange. X type zeolites were found to be more active than Y type zeolites. This behaviour was discussed in terms of the nonoccupancy of cation sites and Lewis acid sites.

This study was extended to include various cation exchanged bleaching earths. The ability of the various cations in imparting activities for the adsorption of  $\beta$ -carotene is indicated as follows;  $\text{H}^+ \sim \text{Fe}^{3+} \sim \text{Mg}^{2+} > \text{Ca}^{2+} > \text{Na}^+$ . The activities were attributed to the acid centres and transition metal ions like  $\text{Fe}^{3+}$  and  $\text{Cu}^{2+}$  on the clay surfaces. There was a linear increase in the activity with the increase in the extent of exchange.

Cation exchanged bleaching earths were also used to bleach palm oil under standard conditions. The results showed that the



bleaching earth has two important functions. First, the removal of colouring bodies in the palm oil and second, the removal or "cleansing" of impurities like peroxides, phosphatides and heavy metals. It was also found that the activities of the cation exchanged bleaching earth for colour reduction and impurities "cleansing" follow the same trend; that is  $H^+$ ,  $Fe^{3+}$  and  $Mg^{2+}$  ions impart high activities whereas  $Ca^{2+}$  and  $Na^+$  ions impart less activities to the bleaching earth.

## CHAPTER 1

### INTRODUCTION

#### 1. Objective

Of all the processes involved in the refining of palm oil, colour bleaching of the oil is the least understood. Although in practice, the process is straight-forward and easy to effect, the actual mechanism involved whereby the pigments and other impurities are removed remains unsolved. Recently, an organised preliminary investigation into this subject was reported (1). It was reported that in addition to physical adsorption of colour bodies, processes involving chemisorption and subsequent chemical reactions occur during bleaching. Reactions involving oxidation and partial isomerisation of carotenoids were suggested(1,2).

The present work is to investigate the nature of active sites present in the bleaching earths that are responsible for the chemisorption of colour pigments in palm oil. It was suggested that cations on the surface of clay such as  $\text{Fe}^{3+}$  served as the active sites for chemisorption (1). However, clays are formed by natural processes and ultimately complex in nature.

Further, they are often not well characterized and occurred as a mixture of a number of clay minerals. Therefore, a model system using zeolite as the adsorbent is used. Zeolite has well characterized crystalline aluminosilicate framework. Zeolite and clay have similar structural characteristics like porosities, high surface areas and more importantly the presence of exchangeable cations in their crystal lattices. Zeolite with exclusively one type of cation can be prepared relatively easily and hence the activity of various cation forms of zeolite towards  $\beta$ -carotene can be deduced without uncertainty.

Bleaching earths ion exchanged with various cations are also prepared and their activities towards bleaching of  $\beta$ -carotene and palm oil were also investigated. The probable active sites present in zeolite and bleaching earth are identified.

An attempt will also be made to identify the type of products formed during the chemisorption of  $\beta$ -carotene by cation exchange zeolite and bleaching earth.

## 2. Refining of Crude Palm Oil

The refining of crude palm oil usually involves a number of basic steps; free fatty acid removal (deacidification), colour removal (bleaching) and deodorisation. The purpose of these processes is to reduce the impurities in the crude oil like

free fatty acid (FFA), phosphatides, colouring matters, various flavour bodies, water and traces of metals to certain levels so that a bland and stable oil suitable for edible purposes is produced. Currently, two conventional refining processes are known to be in operation in Malaysia. These are the alkali-refining process and the physical (steam) refining process.

In the alkali-refining process, the crude palm oil was initially treated with dilute sodium hydroxide solution to remove the free fatty acid. The resulting products after the neutralisation process are neutralised oil and soapstock. However, prior to this step, the crude oil was pretreated with 0.1% phosphoric acid to aid in the removal of phosphatides in the neutralisation process. The neutralised oil is then treated with 1-2% of activated bleaching earth in the bleaching process. The oil is usually bleached under vacuum at a temperature of 90-130°C for 20-40 minutes followed by filtration. In this process the colouring substances with some other impurities are removed. Deodorisation is the final process in the refining of oil whereby the odours and flavours of the oil are removed together with some peroxides, aldehydes, ketones, colouring substances and free fatty acids. The process is carried out under vacuum and the oil is steam-stripped at 200-250°C in the deodoriser.

The main difference in the physical refining process is that the deodorisation and deacidification of the oil are accomplished

in one step. The crude palm oil is first pretreated with a suitable quantity of phosphoric acid and bleached with activated earth in the usual manner. The bleached oil is subsequently deacidified and deodorised in a single step by steam distillation under vacuum at 240-260°C. During this process, free fatty acids, odours and flavours of the oil are removed to produce a completely refined oil.

In the refining of crude palm oil, regardless of which of the refining processes is adopted, the bleaching of the oil with activated earth is an essential and important step.

(a) Bleaching of Palm Oil

Bleaching in general is regarded as the process whereby the colour of the oil is partially or completely removed (3,4). Besides decolourisation of the oil, the process of bleaching also removes phosphatides, soaps, traces of metals and decomposes oxidative breakdown products such as peroxides.

The orange to red colour of palm oil is mainly due to the presence of carotenoids. The average concentration in Malaysian palm oil is in the range of 500-700 ppm. The major fraction of the carotenoids consists of the hydrocarbon carotenes and to a lesser extent the oxygenated carotenoids. The hydrocarbon carotenes are  $\alpha$ ,  $\beta$ ,  $\gamma$ - carotenes and the most important is the  $\beta$ -carotene. Oxygenated carotenoids known as xanthophylls for example 3, 3' dioxo- $\alpha$ -carotene is present in palm oil.

The long conjugated carbon-carbon double bonds in these molecules are unstable and therefore they are readily bleached. During bleaching, carotenoids very likely undergo a number of reactions. They are unstable to heat; thermal degradations are reported to occur above  $200^{\circ}\text{C}$  in nitrogen or vacuum (5,6). Volatile degradation products consist of ionene, 2,6-dimethylnapthalene, m-xylene and toluene. However non-volatile products such as anthracene, methyl-anthracene, pyrene, dimethylpyrene and benzpyrene make up the major fraction (7). These products are formed from intramolecular cyclisation reaction.

Carotenoids are also very unstable in the presence of oxidising agents and acids but stable to alkali. In chemical refining, decolourisation is effected through the destruction of carotenoids by employing oxidising agents such as hydrogen peroxides (8). However, even without oxidising agent, they undergo oxidation when exposed to air particularly in the presence of light. Hence, a solution of carotenes on standing in the presence of light gradually fade practically to a colourless state. The dissolution of carotenoids in vegetable oil however seems to stabilise them towards oxidation.

Carotenoids are very susceptible to cis-trans isomerisation, when exposed to light with or without catalyst, when heated in the dark, when in contact with active surface ( $\text{Al}_2\text{O}_3$ ) and during

treatment with acids (9). For example when trans  $\beta$ -carotene in benzene or hexane is heated in diffused day light isomerization to the mixed cis-trans isomers in the 9 or 13 position occurred (10).

(b) Bleaching Earths

Bleaching earths are clays which in their natural state or after chemical or physical activation have the ability to adsorb colouring matters from oils (11). They are often classed as Fuller's earths and bentonites. Fuller's earth represent a variety of clay which in its natural form has the ability to remove colouring matters. The major clay minerals present in Fuller's earths are attapulgite and sepiolite (8). Minor constituents consist of montmorillonite, kaolinite and illite. Such earths do not respond favourably to acid activation and are used for bleaching in their natural form.

Bentonites is the geological term for clays that are produced by the devitrification of volcanic ash (12). However, mineralogically, bentonites are actually 75 per cent or more of the clay mineral montmorillonite (8). Minor constituents are kaolinite, illite, mica and traces of other minerals. Bentonites in nature also possess substantial decolourising power, but in most cases the ability to decolorise is too low to be commercially useful. To improve on this property the clays are usually acid activated. After this treatment, they exhibit high decolourising ability comparable to Fuller's earths and in some instances even better.

(i) Structure of Montmorillonite

Most clay minerals are built up from two basic structural units. One unit consists of two sheets of closely packed oxygens or hydroxyls in which aluminium atoms are embedded in an octahedral coordination so that they are equidistant from six oxygens or hydroxyls (Figure 1.1). This is the gibbsite unit where only two-thirds of all the possible octahedral positions are filled to balance the structure and has the formula  $Al_2(OH)_6$ . The thickness of this unit is  $5.05\text{\AA}$ .

The second unit consists of silica tetrahedrons. In each tetrahedron a central silicon atom is equidistant from 4 oxygens or hydroxyls. They are arranged to form a hexagonal network which is repeated indefinitely to form a sheet of the composition  $Si_4O_6(OH)_4$  (Figure 1.2). The tetrahedrons are arranged so that their tips are all pointed in the same direction and the bases of all the tetrahedrons are in the same plane. The silica unit has a thickness of  $4.93\text{\AA}$ .

The structure of montmorillonite consists of a central gibbsite layer sandwiched between two silica sheets to form a structural unit (13) (Figure 1.3). All the tips of the tetrahedrons of the silica layers point towards the center of the unit. The silica and gibbsite sheets are combined so that the tips of the tetrahedrons of each silica sheet and one of the oxygen of the octahedral sheet form a common layer. The octahedral oxygens which



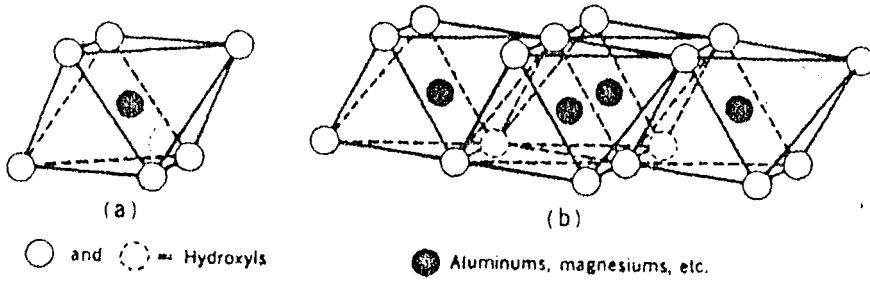


Figure 1.1: (a) A single octahedral unit and  
(b) The sheet structure of the octahedral units.

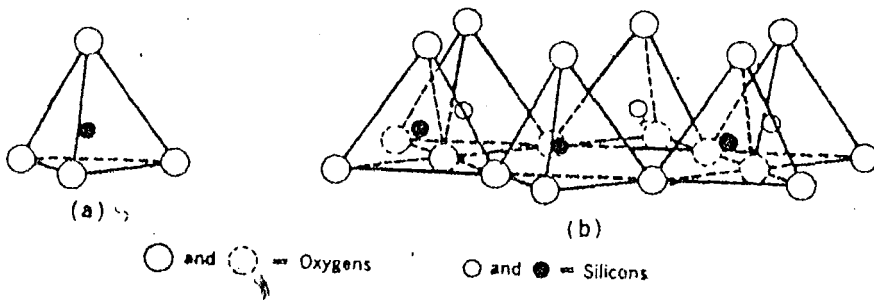


Figure 1.2: (a) A single silica tetrahedron and  
(b) The sheet structure of silica tetrahedra  
arranged in a hexagonal network.

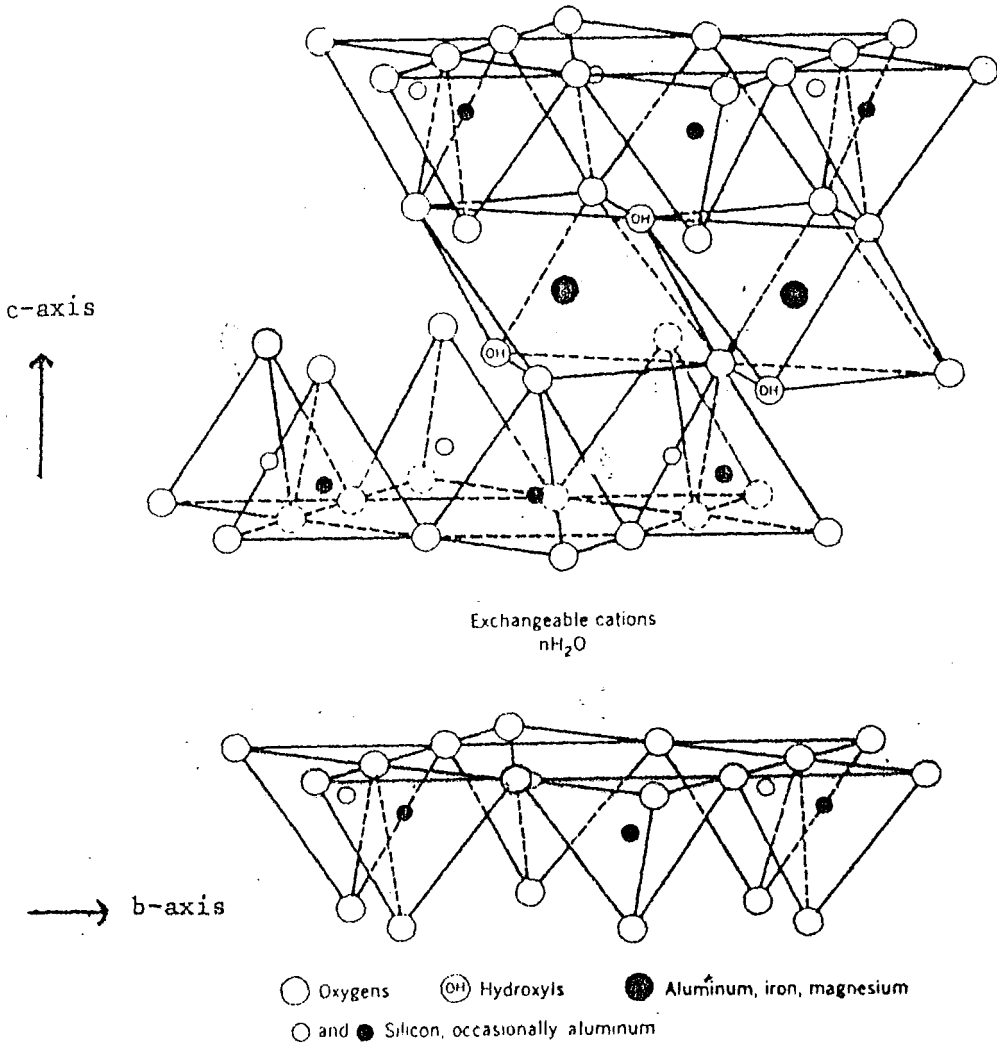


Figure 1.3: Arrangement of Octahedral and Tetrahedral  
Sheets to form the Montmorillonite Structure

are not shared with the silica sheets become hydroxyls. The layers are continuous in the a and b directions and are stacked one above the other in the c direction.

In the stacking of the silica-alumina-silica units the oxygen layer of each unit are adjacent to oxygen of the neighbouring units. As a consequence there is a very weak bond and an excellent cleavage between them. Water and other polar molecules such as glycol and methanol can enter between the unit layers causing the lattice to expand in the c-direction. As a result the c-axis of montmorillonite is not fixed but can vary from  $9.6\text{\AA}$  to  $21.4\text{\AA}$  (8).

The theoretical formula of montmorillonite is  $(\text{OH})_4\text{Si}_8\text{Al}_4\text{O}_{20}\cdot n\text{H}_2\text{O}$  and the theoretical composition is  $\text{SiO}_2$ , 66.7 per cent;  $\text{Al}_2\text{O}_3$ , 28.3 per cent;  $\text{H}_2\text{O}$ , 5.0 per cent. However, in actual case, the formula always differs from the theoretical one because of lattice substitution. In montmorillonite, substitutions occur mainly within the octahedral layer, where magnesium or iron replaced aluminium and to a much lesser extent (< 15 per cent) substitution of silicon by aluminium in the tetrahedral sheets can occur. Substitutions in the octahedral sheet may vary from few to complete.

The proxying of aluminium for magnesium or iron unbalanced the lattice and the net positive charged deficiency in montmorillonite is about 0.66 per unit cell. The charge deficiency in the crystal

lattice is balanced by exchangeable cation adsorbed between the unit layers and around their edges. The cation exchange capacity for montmorillonite is about 80-120 milliequivalent per 100g (14) and about 80 per cent or more of this value arise because of substitution in the crystal lattice. Broken bonds are responsible for the less than 20 per cent of the cation exchange capacity. Broken bonds around the edges of the structural units would give rise to unsatisfied charges and are balanced by adsorbed cations. The contribution to ion exchange capacity by broken bonds would increase as the particle size decreased.

(ii) Acid Activation of Montmorillonite

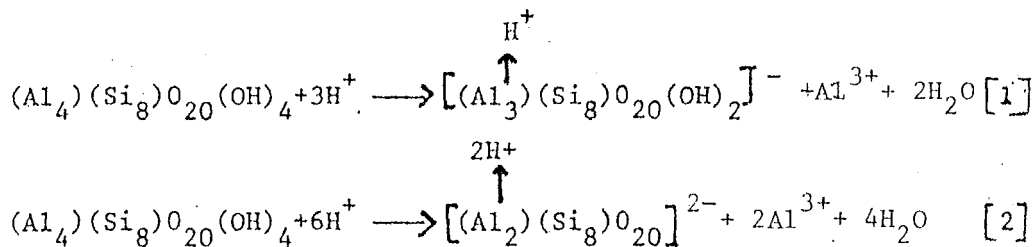
In acid-activation process the clay is slurried with sulphuric or hydrochloric acid for some time at a moderately elevated temperature. Following this, the slurry is washed, dried, calcined and prepared in the desired particle size distribution (12).

In practice, only certain types of montmorillonite clays are activable by acid treatment. Usually, low-swelling montmorillonites with high ratio of soda to lime and appreciable cation exchange capacity react satisfactorily to acid activation (8)

During acid treatment, the exchangeable alkali or alkaline earth cations are partially or completely replaced by hydrogen ions.

The protons also penetrate the octahedral part of the crystal lattice displacing magnesium, iron and aluminium ions in about that order. The attack by protons is reasoned to be most probably first at the edges of the platelets and then proceed into the interior of the crystal structure. Magnesium, iron and aluminium ions displaced from the octahedral positions proceed to exchange sites and then into solution (12). The removal of tetrahedral coordinated cations is minimum or none at all (15).

The changes that occurred on acid leaching of an idealised montmorillonite may be expressed as:



At this stage [2], half of the aluminium atoms have been removed from the structure together with two hydroxyl groups. The remaining aluminium atoms are tetrahedrally coordinated with the four remaining oxygen atoms (16) (Figure 1.4). The change from octahedral to tetrahedral coordination leaves the crystal lattice with a negative charge which is balanced by a hydrogen ion. If acid treatment is allowed to proceed further, greater dissolution of octahedral aluminium would occur until eventually the whole crystal structure is destroyed.

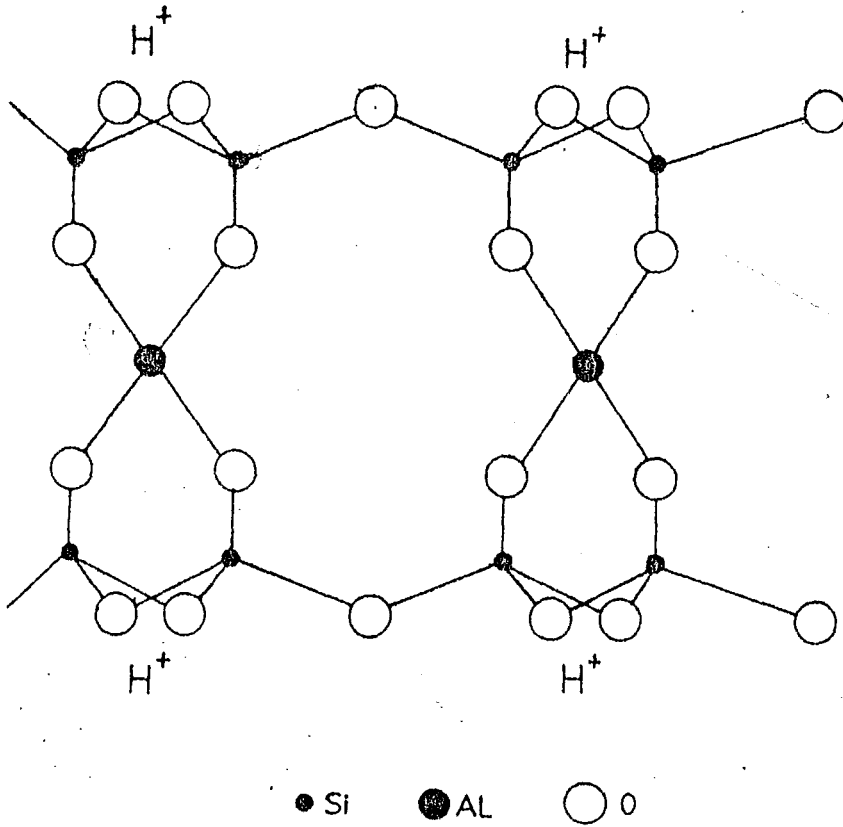


Figure 1.4: Idealized Structure of Acid-Activated Montmorillonite

In essence, acid activation serves to increase surface area, porosity and the acidity of the clays which are important factors in the bleaching of oils (12, 18, 19).

### 3. Zeolites

Zeolites have been the subject of a great deal of research especially during the past decade. A large volume of works dated back to the 1950s was found in literature mainly dealing with their syntheses and properties as adsorbents. Zeolite minerals were first discovered in 1756 by Baron Cronstedt, the Swedish mineralogist (20). Although, the properties of these minerals such as ion exchange, reversible dehydration and selective adsorption of gases and other molecules were also discovered not long afterwards, these properties were not understood by early scientists. In 1930s, the advent of X-ray diffraction techniques (21, 22) had enabled a more positive identification of their structures and compositions which eventually led to a better understanding of the various properties of zeolites.

The introduction of X-ray diffraction has given a new impetus in the research of zeolites. In the years between 1940s-1960s, a number of scientists in particular R.M. Barrer, R.M. Milton, D.W. Breck and their co-workers successfully synthesized and characterized a number of zeolites. They were mordenite (23) type A (24), type X and type Y zeolites (20, 25). Today, these

zeolites are very important especially in the field of heterogenous catalysis.

In the subsequent years, a tremendous amount of research was done which was directed almost exclusively to their adsorption properties. The structural properties of zeolite allowed selective adsorption of traces of impurity from gases and fluids and also selective removal of one component from a mixture based on molecular size differences. Consequently zeolites were developed for a wide variety of purification and separation processes. Important industrial applications of zeolites as adsorbent include the removal of water, carbon dioxide and various sulphur compounds in the purification of air, natural gas and hydrocarbons for various chemical reactions (26). The other important use was in the separation of hydrocarbons. By using zeolite of proper size, the n-paraffins were separated from branched and cyclic hydrocarbons in a mixture. Zeolite was also used to separate para-xylene from a mixture of xylene and ethyl benzene. The para-xylene was used as raw material for polyester production.

In recent years, the discovery that these zeolites possess catalytic activity added a new dimension to the research on zeolite surfaces. Their catalytic activities have the most important application in modern oil refining and in the petrochemical industry. In addition to catalysing cracking reactions, they were used in



hydrocracking, isomerisation of aromatic hydrocarbons and dehydration of alcohols.

The reason for this wide range of application for the zeolites was because they could be easily tailored for specific and desired purposes. They were a unique class of aluminosilicate which were characterized by a highly ordered and uniform crystal structure. They have uniformly small sized pores leading from exterior surface to an internal three dimensional cagework. These pores can be manufactured with precision ranging from 3 to 10Å. Consequently adsorption can take place internally as well as externally. They also have strong affinity for polar or polarizable molecules, combined with the high surface area allow for the process of purification and separation. The adsorption and catalytic activity can also be modified by ion exchange with cations to provide a nearly limitless variety of products and potential uses.

(a) Crystal Structure of X and Y Zeolites

Zeolites can be considered as crystalline three-dimensional cross-linked polymers. The basic structural units are silicon and aluminium atoms which are tetrahedrally coordinated with four oxygen atoms to form  $\text{Si}(\text{O}/2)_4$  and  $\text{Al}(\text{O}/2)_4$  tetrahedra (20,25). The O/2 represents the bridging oxygen mutually shared between two tetrahedral units contributing one of the two valence charges of each oxygen to each tetrahedron. Since aluminium atoms

are trivalent, the aluminium oxygen tetrahedron will each formally bear one unit negative charge. The charge of these units is satisfied by cations such as  $\text{Na}^+$ ,  $\text{K}^+$ ,  $\text{Ca}^{2+}$  or  $\text{Mg}^{2+}$  present in the framework thus making the crystal electrically neutral.

The three-dimensional tetrahedra are arranged in a definite geometric form. The X and Y zeolites belong to the faujasite type of structure that based on the stacking of the cubooctahedral cages usually called the sodalite cages. Each sodalite cage consists of eight hexagonal faces, six square faces, 24 vertices and 36 edges (27). (Figure 1.5a). In X and Y zeolites, these cages are stacked in a tetrahedral array, that is, the cubooctahedra are joined at the octahedral faces by hexagonal prisms (Figure 1.5c). The lattice generated is a face-centred cubic with octahedral symmetry. The lattice constant for sodium form of hydrated X zeolite with a Si/Al ratio of 1.25 is  $24.93\text{\AA}$  and hydrated Y zeolite with Si/Al ratio of 2.5 is  $24.66\text{\AA}$ . The typical unit cell composition of hydrated X and Y zeolites are  $\text{Na}_{86}[(\text{AlO}_2)_{86}(\text{SiO}_2)_{106}] \cdot 264\text{H}_2\text{O}$  and  $\text{Na}_{56}[(\text{AlO}_2)_{56}(\text{SiO}_2)_{136}] \cdot 264\text{H}_2\text{O}$  respectively.

The volume enclosed by the tetrahedral array of sodalite cages is a large void referred to as the supercage. (Figure 1.5b) which are also stacked in a tetrahedral array and are interconnected by rings of 12 tetrahedra. In general, a supercage is connected to four sodalite cages by rings of six tetrahedra which

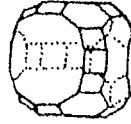


Figure 1.5a: Sodalite Cage

Figure 1.5b Supercage of Faujasite Type

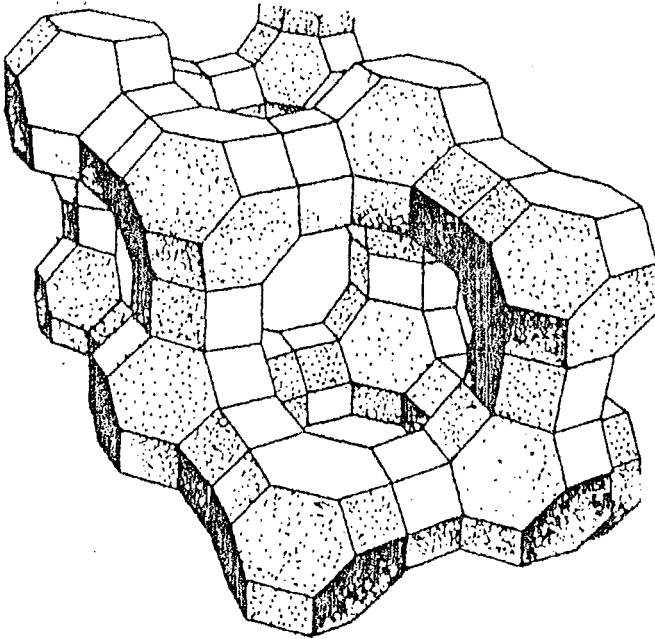


Figure 1.5c: Arrangement of Sodalite Cages to give Faujasite Structure.

are also the walls between the large and small cages. The sodalite cages are linked by six oxygen atoms through adjacent ring of six tetrahedra. Therefore, there are actually two independent three-dimensional network of cavities; one of sodalite cages interconnected by double rings of six tetrahedra and one of supercages linked by sharing ring of 12 tetrahedra; both interconnected by rings of six tetrahedra. The access into these cavities is governed by the dimensions of the largest rings.

(b) Properties of X and Y Zeolites

Although many factors influence the properties of zeolites, the three most important are the open framework structure and its attendant pore size, the Si/Al ratio and the exchangeable cations.

The openings or pores in the framework are important since they must be larger than the adsorbate or the reactant molecules, so as to allow these molecules to freely diffuse to and from the internal surfaces. Selective adsorption exhibits by the dehydrated zeolites in many cases is directly related to the pore size (28). However X and Y zeolites have relatively large pores in the range 7-9 Å which is usually large enough for most molecules to enter.

The greater the Si/Al ratio, the fewer the number of cations per unit cell which will result in a much greater stability of the crystal lattice (29). Therefore Y zeolite which has a greater

Si/Al than X zeolite can withstand higher temperature, more stable to acids and can ion exchange with many cations without loss in crystallinity. The greater stability of the cations inside the structure also resulted in Y zeolite having higher catalytic activity and stronger solid acidity (29, 30).

The catalytic and adsorption properties of zeolites are very often modified by the type of cations in the crystal lattice. The cations in the zeolites can be easily exchanged with other cations simply by digesting the zeolites in an aqueous solution of the appropriate cation. In general, the cation exchange process is dependent upon the nature of the cation species, i.e. the size and charge of the cation (31, 32) the type of zeolite structure (33, 34, 35), the temperature and the cation concentration of the solution (36,37). Furthermore the amount of breakdown in the ion exchanged sample is influenced by both the pH and the ion concentration of the solution used for ion exchange (30, 38).

The molecular-sieve properties of zeolite may be altered by exchanging larger or smaller cations for cation that block the channels or by removing a cation from the channel by introducing one divalent cation for two monovalent cations. For example, the replacement of sodium ion by potassium ion in synthetic zeolite A causes the adsorption of  $O_2$ ,  $CH_3OH$ ,  $C_6H_6$  and  $C_2H_2$  (39) to decrease to essentially zero. The adsorption of

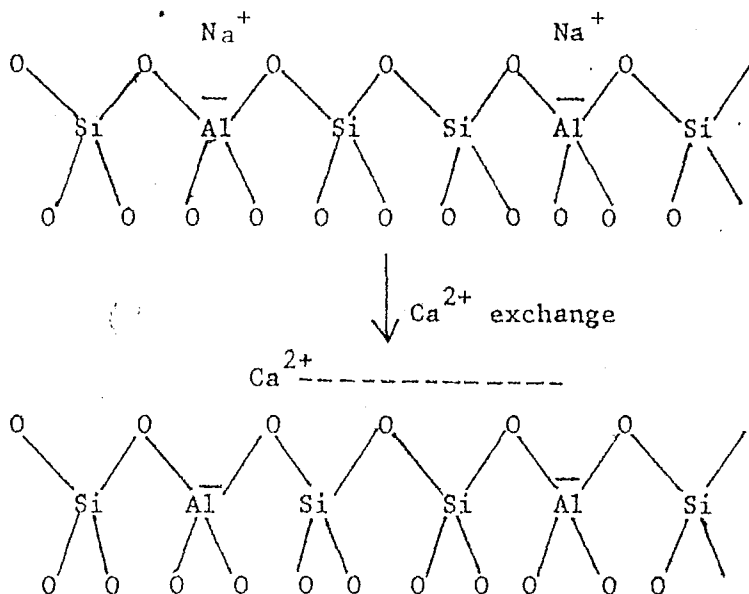
$N_2$ ,  $nC_6H_{14}$  and  $C_3H_8$  in the same zeolite increases from zero to substantially higher value when calcium ions replaced the sodium ions (39). Replacement of the sodium ions by the larger potassium ions partially blocked the opening into the cavities sufficiently to exclude  $O_2$  and the other molecules whereas with the replacement of two sodium ions by a divalent cation, the channels are no longer blocked with cations and normal hydrocarbons become adsorbable.

Catalytic activity of zeolites can also be significantly modified by the process of cation exchange. The seat of this catalytic activity in the zeolites has been the subject of considerable study and speculation and it is attributed to the electrostatic fields associated with the polyvalent cation (40, 41), strong hydrogen (Bronsted) acids (42-47) and incompletely coordinated aluminium ions (Lewis acids) (48,49). The mechanism for the formation of these catalytic active sites as a result of cation exchange will be discussed briefly in the following passages.

#### (i) Electrostatic Fields

In univalent cationic form of zeolite, for example sodium zeolite, the negative charge in each alumina tetrahedron is balanced by a closely associated sodium cation. Consequently, the crystal lattice is electrically neutral. When two sodium ions are exchanged for a divalent let say calcium ion, the calcium

ion will be assymmetrically located with respect to the two alumina tetrahedra as shown in Y zeolite.



This is because the two alumina tetrahedra are some distance apart especially in zeolite with high Si/Al ratio. In this position, one of the positive charges on the cation is balanced by the negative charge on the nearest alumina, leaving an excess of one positive charge at the cation site. The bond which associates the cation and the next alumina is long and weak, consequently, virtually a full negative charge exists at this site. Therefore a strong dipole is created and was shown (40) by theoretical calculations to have sufficient energy to strongly polarise the C-H bond which is an essential condition in catalytic reaction involving carbonium ion mechanism.

## (ii) Bronsted and Lewis Acidities

Bronsted acidity associated with polyvalent cations arises from the partial hydrolysis of the polyvalent cations by





Thus one structural hydroxyl group is formed for every two exchange sites. At higher calcination temperature, dehydroxylation reaction (removal of  $H_2O$  from framework) begins to occur and the Bronsted acidity is converted to Lewis acidity with the formation of tricoordinated aluminium ion. In general, it seems that maximum Bronsted acidity developed between calcination temperature of  $450^{\circ}C - 600^{\circ}C$  depending on the type of zeolite concerned (50). Above calcination temperature of  $600^{\circ}C$  dehydroxylation of the zeolite occurs and Lewis acid sites are formed at the expense of the Bronsted sites (46, 55). Consequently, the catalytic activity of zeolite increases with the increase in the extent of cation exchange. The higher the Si/Al ratio, the greater is the electrostatic field in the zeolite which results in greater hydrolysis of the hydrated cation. The cation itself also promotes the formation of the acid sites by polarising the adsorbed water (46) so that dissociation occurs. The smaller the ionic radius of the cations, the greater is the polarising effect.

Another way Bronsted acidity can be introduced into the zeolite is by first exchanging the zeolite with ammonium ions. The ammonium ion is then decomposed by heat to ammonia (deammoniation) and the proton liberated reacts with the framework oxygen to form a hydroxyl group (51, 52, 53). The reactions are as follows: